MODELING AND EMPIRICAL RESEARCH ON ENERGY PARTITIONING OF REGIONAL SEISMIC PHASES USED FOR EXPLOSION MONITORING

Mark D. Fisk[1], Thorne Lay[2], and Steven Taylor[3]

ATK Mission Research[1], University of California, Santa Cruz[2], and Los Alamos National Laboratory[3]

Sponsored by National Nuclear Security Administration
Office of Nonproliferation Research and Engineering
Office of Defense Nuclear Nonproliferation

Contract Nos. DE-AC52-04NA25536[1], DE-FC52-04NA25537[2], and W-7405-ENG-36[3]

ABSTRACT

We are investigating energy partitioning of local and regional seismic phases, focusing on geophysical causes of their frequency dependence and variances, mechanisms of P-to-S conversion, different scattering effects for P and S phases that affect their complexity, and implications for reliable and defensible use of P/S discriminants. For empirical studies, we are using large data sets consisting of Pn, Pg, Sn and Lg spectra and time-domain measurements at frequencies from 0.1 to 10 Hz, and correcting for geometrical spreading, attenuation, and magnitude, so that the variability and frequency dependence of individual phases may be assessed. Objectives are to quantify these aspects for explosions and earthquakes near the Lop Nor, Semipalatinsk, Novaya Zemlya, and Nevada test sites, and assess whether consistent patterns emerge. We plan to interpret empirical observations in terms of geophysical mechanisms by using complex elastic-screen simulations, spanning relevant spectral content (0.1 to 10 Hz) for distances of at least 0 to 600 km, using realistic models with multi-scale heterogeneity, rough Moho, topography, and other boundaries.

Preliminary efforts have focused on examining spectral scaling as a function of source size and frequency-dependent P/S discrimination performance for nuclear explosions and selected earthquakes near the Lop Nor test site in China. Network-averaged relative spectra for given phases (using nearby events of various sizes) are compared to theoretical relative spectra using a modified Brune (1970) model for earthquakes and a Mueller and Murphy (1971) model [MM71] for explosions in granite. Spectral contributions of surface reflected phases are also considered. Some preliminary observations are as follows. First, a modified Brune model, with corner frequency scaling as seismic moment to the -1/4 power, seems to adequately predict spectral scaling for the earthquakes examined. Evidence that Pn, Sn and Lg from earthquakes scale fairly similarly with source size suggests that frequency dependence of P/S discrimination performance is not primarily due to earthquake source mechanisms. Second, a modified MM71 model, that treats surface-reflection interference, provides reasonably good fits up to about 4 Hz to empirical spectral ratios of P and Pn waves for Lop Nor explosions, if they are suitably averaged over stations and azimuths. Spectral interference effects due to surface reflections appear to be significant for teleseismic and regional phases. For Lop Nor explosions between mb 4.7 to 6.5, the main effect of destructive interference occurs between about 0.7 to 2.5 Hz. Frequency-dependent discrimination performance of Pn/Sn and Pn/Lg appears to be mainly due to differences in corner frequencies of P and S waves and spectral overshoot for explosions, as observed by Xie and Patton (1999). Enhanced relative energy of Sn and Lg is observed at frequencies below about 2 Hz for the shallower 1996/07/29 tunnel shot, relative to the 1996/06/08 shaft shot, as compared to MM71. It appears that corner frequencies, depth of burial, and interactions with the free surface all have significant impacts, to varying degrees, on the frequency dependence of P/S discriminants for explosions. Path and station effects that impact the variability of regional phases are being explored.

OBJECTIVES

This is a 3-year contract to investigate energy partitioning of local and regional seismic phases to better understand geophysical causes of the variability and frequency dependence of P/S discriminants. We are analyzing large data sets of Pn, Pg, Sn and Lg spectra and time-domain measurements at frequencies from 0.1 to 10 Hz, and correcting for geometrical spreading, attenuation, and magnitude, so that the variability and frequency dependence of individual phases may be assessed. Objectives are to quantify these aspects for explosions and earthquakes near the Lop Nor, Semipalatinsk, Novaya Zemlya, and Nevada test sites, and assess whether consistent patterns emerge. We plan to interpret empirical observations in terms of geophysical mechanisms by using complex elastic-screen simulations, spanning relevant spectral content (0.1 to 10 Hz) for distances of at least 0 to 600 km, considering realistic models with multi-scale heterogeneity, rough Moho, topography, and other boundaries.

RESEARCH ACCOMPLISHED

Preliminary efforts have focused on spectral modeling of Pn, Sn, and Lg phases for nuclear explosions and selected earthquakes near the Lop Nor test site in China. This initial study region has the benefit of including many nearby explosions and earthquakes that were recorded by numerous regional stations, allowing much of the path variability to be averaged out to better examine source characteristics. Network-averaged relative spectra (using nearby events of different sizes) are compared to theoretical relative spectra, using a modified Brune (1970) model for earthquakes and a Mueller and Murphy (1971) model [MM71] for explosions in granite. Spectral contributions of surface reflected phases are also considered. Below we describe the earthquake and explosions models, present some example of spectral scaling, and draw some conclusions regarding near-source mechanisms that affect P/S discrimination.

Brune Earthquake Source Model

The Brune (1970) model is used here to represent the source spectral function for earthquakes. For a particular phase type, ξ (P or S), the spectrum is given by

$$S_\xi(f) = \frac{M_0 R_{\theta\phi}(\xi)}{4\pi\sqrt{\rho_s \rho_r v_s(\xi)^5 v_r(\xi)}[1 + (f/f_c(\xi))^2]} \quad , \tag{1}$$

where M_0 is the seismic moment, $R_{\theta\phi}$ is the radiation pattern coefficient for P or S waves, ρ_s and ρ_r are the source and receiver medium densities, v_s and v_r are the source and receiver medium velocities for P or S waves, and f_c is the source corner frequency. For this study, the parameters in Table 1 of Taylor et al. (2002) are used for the radiation pattern coefficients, densities, and velocities. For a Brune (1970) dislocation source, the corner frequency is given by

$$f_c(\xi) = c_\xi v_s(\xi)\left(\frac{\sigma_b}{M_0}\right)^{1/3} \quad , \tag{2}$$

where σ_b is the stress drop and c_ξ is a constant that can depend on phase type. In the following, $c_P = 0.41$ and $c_S = 0.49$ are used. Taylor et al. (2002) discuss observations by Cong et al. (1996), Nuttli (1983), and Mayeda and Walter (1996) suggesting that the scaling of corner frequency as event moment (M_0) to the -1/4 power is more appropriate than -1/3 scaling for earthquakes in central Asia and the western U.S. This departure from cube root scaling can be viewed as a result of non-constant stress drop. Following Walter and Taylor (2002), non-constant stress drop may be treated by defining the apparent stress drop for a given event moment, M_0, as

$$\sigma_b = \sigma_b^{(0)}\left(\frac{M_0}{M_0^{(0)}}\right)^{\psi} , \tag{3}$$

where $\sigma_b^{(0)}$ is the stress drop at a reference moment $M_0^{(0)}$. This formulation of the apparent stress drop provides appropriate units for any scaling exponent ψ. Values of $\psi = 0$ and $\psi = 1/4$ correspond to corner frequency scaling with moment to the -1/3 and -1/4 powers, respectively. Although there are some trade-offs, the parameters $\sigma_b^{(0)}$, $M_0^{(0)}$, and ψ may be fit to data. Setting $\log M_0^{(0)} = 15.0$ Nm and restricting $0 < \psi < 0.25$, the best fit obtained for the Lop Nor earthquakes presented below is for $\psi = 0.21$ and $\sigma_b^{(0)} = 3.58 \times 10^6 \mathrm{N/m}^2$.

Mueller/Murphy Explosion Source Model

Mueller and Murphy (1971) represented the radial stress by a Heaviside step function and an exponentially decaying term, $\sigma_{rr} = -(P_0 + P_1 \exp(-\omega_1 \tau))U(\tau)$, for the pressure profile acting at the elastic radius. Under this assumption, the far-field amplitude spectrum (without geometrical spreading term) is given by (e.g., Denny and Johnson, 1991)

$$|S(\omega)| = \frac{\gamma P_p R_e \sqrt{\omega^2 + (\omega_1 P_0 / P_p)^2}}{\rho_s v_s(P) \sqrt{\omega^2 + \omega_1^2} \sqrt{(\omega_0^2 - \gamma\omega^2)^2 + \omega_0^2 \omega^2}}, \quad (4)$$

where $\sqrt{\gamma} = v_s(P)/2v_s(S)$, R_e is the elastic radius, proportional to $W^{1/3}(\rho g h)^{-0.417}$ for granite (from empirical studies), h is the depth of burial, and the corner frequency is $\omega_0 = v_s(P)/R_e$. Mueller and Murphy (1971) inferred that the peak pressure is 1.5 times the overburden, i.e., $P_p = P_0 + P_1 = 1.5\rho g h$, and assuming incompressibility, $P_0 = (4\mu/3)(R_c/R_e)^3$, where empirical studies indicate that $R_c = cW^{0.29}h^{-0.11}$ for granite. This model is used with source medium density and velocities inferred from geological borehole samples at the LNTS reported by Matzko (1994). The density is set at 2620 kg/m^3, and the P and S wave velocities (all in units of m/s) are set at 5300 and 3300 for explosions shallower than 500 m and 5600 and 3500 for the explosions deeper than 500 m. Murphy and Barker (2001) showed that their Shagan River model for explosions in granite (with $\omega_1 = 0$) provides reasonable interpretation of P wave spectra for LNTS explosions between mb 5.0 to 6.2, although they found it necessary to increase the source medium velocities by about 30% for larger/deeper explosions to fit the corner frequency.

As described by many authors (e.g., Lay, 1991; Murphy and Barker, 2001; and references therein), surface reflections, interpreted as pP, can significantly affect amplitudes of teleseismic P at frequencies of destructive and constructive interference. As noted by these authors, this effect is complicated by nonlinear spallation processes. Thus, the relative amplitudes and delay times of pP phases cannot be predicted simply by linear reflection (i.e., the relative amplitudes are generally much lower and the delay time longer than predicted by linear theory), nor are the reflections purely impulsive signals. Nevertheless, the contribution of pP to the observed P wave amplitude spectrum is modeled by

$$\left| \frac{P(\omega) + pP(\omega)}{P(\omega)} \right| = \sqrt{1 + A^2 - 2A\cos(\omega t_0)}, \quad (5)$$

where A is the relative amplitude of pP to P and t_0 is the pP delay time. These parameters cannot be estimated from simple linear reflection theory, but may be estimated directly from network-averaged P wave spectra.

Examples of Relative Spectra and Model Fits

Using the ratio of spectra of a given seismic phase for two nearby events recorded by the same station has the benefit that the majority of path (including attenuation), instrument response, and other station effects are canceled out. Thus, the use of relative spectra, when averaged over numerous stations with good azimuthal coverage, is expected to provide a fairly good estimate of the far field relative source spectra. It is particularly useful to consider nearby events with substantially different source sizes to highlight differences in spectral behavior. For investigation of regional phase spectra, it is most useful to also consider more recent events that were recorded by up to 17 regional stations in

Kazakhstan, Kyrgyzstan, Pakistan, and Russia, most of which were installed (or disseminated data) after mid 1994. LNTS explosions that best meet these criteria are the 1996/07/29 tunnel shot (mb 4.7) and the 1996/06/08 shaft shot (mb 5.8). A drawback is that these events were separated by about 30 km and the emplacement conditions were different. Two shaft shots on 1993/10/05 (mb 5.8) and 1992/05/21 (mb 6.5) are also considered below, although these events have recordings by only 5 common regional stations, all of the Kyrgyzstan network (KNET). The 1999/01/27 (mb 3.95) and 1999/01/30 (mb 5.40) earthquakes are very useful to study because they occurred very close to each other and the LNTS (Figure 1), they both have similar depths of about 20 km, based on well-constrained depth-phase solutions, and the difference in their magnitudes is sufficient to examine effects of source size on the relative spectra.

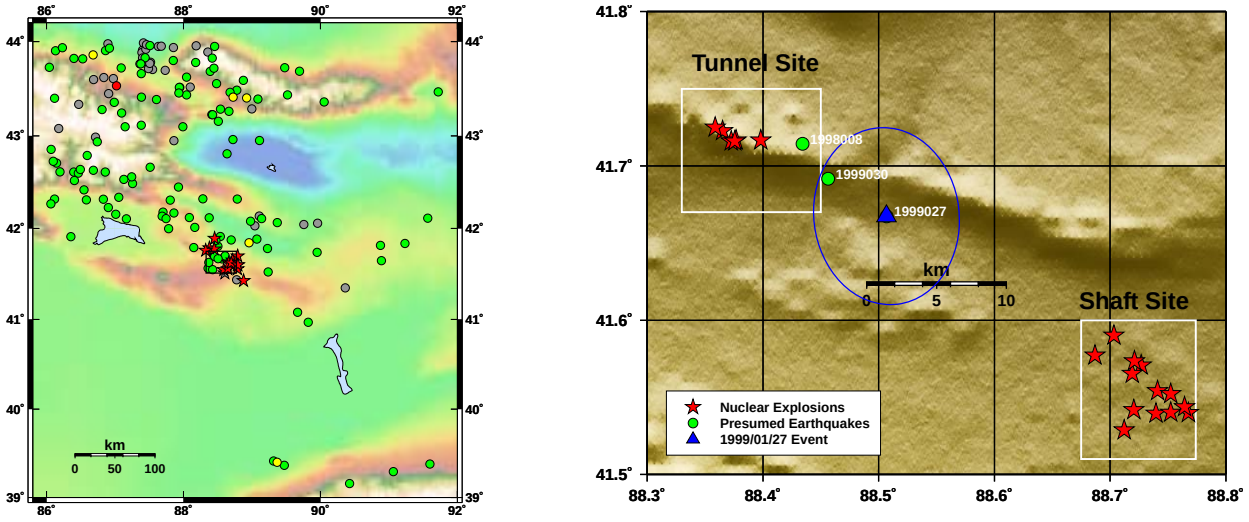

Figure 1. Maps showing locations of nuclear explosions and 156 regional earthquakes considered in this study.

Figure 2 shows network-averaged (using 13 to 17 common stations) relative spectra of Pn, Sn and Lg phases for the pairs of explosions in 1996 and earthquakes in 1999. It also shows the relative spectra of teleseismic P waves for the explosions, using 33 common stations and arrays. Spectra were restricted to a signal-to-noise ratio (SNR) of at least 2.5, and at least 3 stations with adequate SNR are required to contribute to the network average at a given frequency. Last, Figure 2 shows the theoretical relative spectra based on Mueller/Murphy (MM71) and Brune models. Yields and depths of 3 kT and 240 m for the 1996/07/29 shot and 70 kT and 480 m for the 1996/06/08 shot were used. Moments for the earthquakes were computed using $\log M_0 = 1.5 M_W + 16.05$ (Hanks and Kanamori, 1979) and estimates of $M_W = 4.38$ and $M_W = 5.69$ for the 1999 earthquakes. Some observations from Figure 2 include:

- The relative spectra of Pn, Sn and Lg for the earthquakes are all very similar over frequencies of 0.6-3.0 Hz. Variations for different phases outside this frequency range are not very dramatic. Relative spectra for all phases are fairly consistent with the modified Brune model using corner frequency scaling as moment to the -1/4 power.
- Network-averaged P (magenta) and Pn (solid red) relative spectra for the 1996 explosions agree surprisingly well. This is likely achieved because of averaging over many teleseismic or regional stations with fairly good azimuthal coverage. Similarities in the P and Pn relative spectra, including the minimum at about 2 Hz and the local maxima at about 1.2 and 3.5 Hz, suggests that these curves represent relative source characteristics. Significant deviations of these curves from the MM71 curve are explored below.
- Network-averaged Sn (solid green) and Lg (solid blue) relative spectra for the explosions exhibit very significant differences from the P and Pn curves, predominantly at frequencies below about 2 Hz, indicating that Sn and (even more so) Lg energy are enhanced at these lower frequencies for the smaller/shallower explosion in a man-

ner inconsistent with predictions by the MM71 model for P waves. Hypotheses of Rg-to-S scattering and spall effects have been investigated to explain this behavior, which is also observed at other test sites.

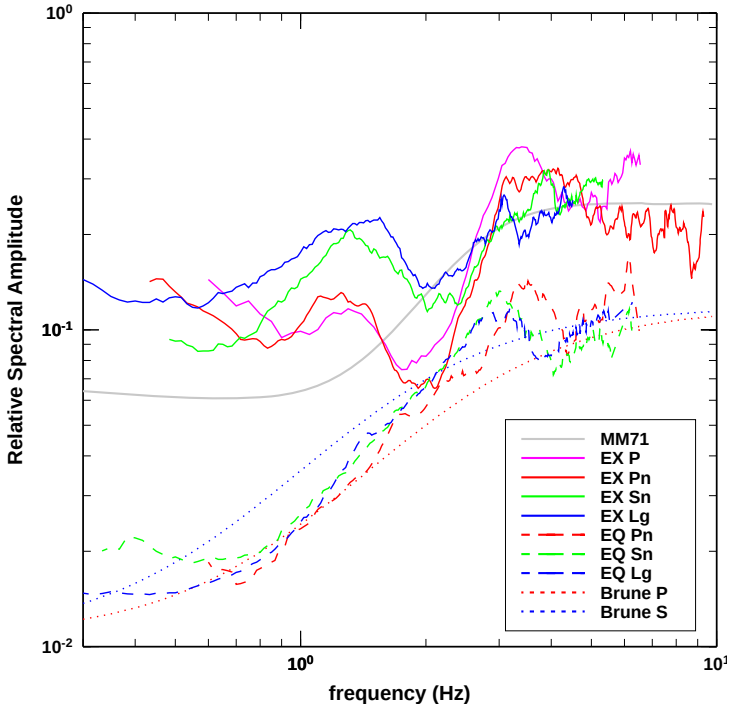

Figure 2. Relative spectra for two 1996 explosions and two 1999 earthquakes (smaller over larger). The legend associates the various curves with theoretical and empirical relative spectra for various events and phase types.

To explore deviations of the P and Pn relative spectra from MM71, Figure 3 shows the result of fitting pP parameters (black curve, MM71 P+pP) to the network-averaged teleseismic P relative spectra (solid magenta) for the 1996 shots. The dotted magenta curves represent the 90% confidence interval of the network-averaged P spectral ratio, indicating considerable variability. The relative amplitudes and delay times are estimated to be 0.49 and 0.47s for the July tunnel shot and 0.13 and 0.90s for the June shaft shot, which are consistent with the range of values obtained for tunnel and shaft shots for LNTS explosions prior 1993 (Murphy, 2005). Treating pP interference accounts for the majority of deviations from the MM71 (P only) model from about 0.8 to 3.5 Hz. The first local maximum in the spectral ratio corresponds to constructive interference for the smaller shot in the numerator. The first local minimum corresponds to constructive interference for the larger shot in the denominator. Differences in theoretical and empirical curves below about 0.6 Hz is likely due to inadequate overshoot in the model used here. The green curves in Figure 3 show spectral ratios for the two 1996 explosions for Pn at MAK (left) and P at EKA (right), which exhibit even more pronounced frequency-dependent departures from the MM71 P-only model. Comparison of these two plots illustrates that these pronounced variations can be observed for both regional and teleseismic phases. Such strong variations at individual stations are often reduced considerably by network averaging because the pP relative amplitudes and delay times vary from one station to another as functions of many geophysical effects, including take-off angle and asymmetric nonlinear spall effects (Murphy, 2005). There are undoubtedly other effects that have not been treated here.

Figure 4 shows similar relative spectra for the 1993/10/05 (mb 5.8) shot to the 1992/05/21 (mb 6.5) shot, both at the shaft site. Yields and depths of 75 kT and 650 m for the 1993 shot and 650 kT and 1000 m for the 1992 shot were used to fit the data. This suggests that the 1993 shot may have been slightly overburied, although there is currently no conclusive evidence. The yield and depth of the 1992 event are consistent with current estimates. The pP relative

amplitudes and delay times are estimated to be 0.42 and 0.69s for the 1993 shot and 0.15 and 1.34s for the 1992 shot. Estimates of pP parameters by Murphy (2005) for the 1992 shot are 0.29 and 1.18s. Modest differences in these estimates could be due to the use of different stations and processing methods.

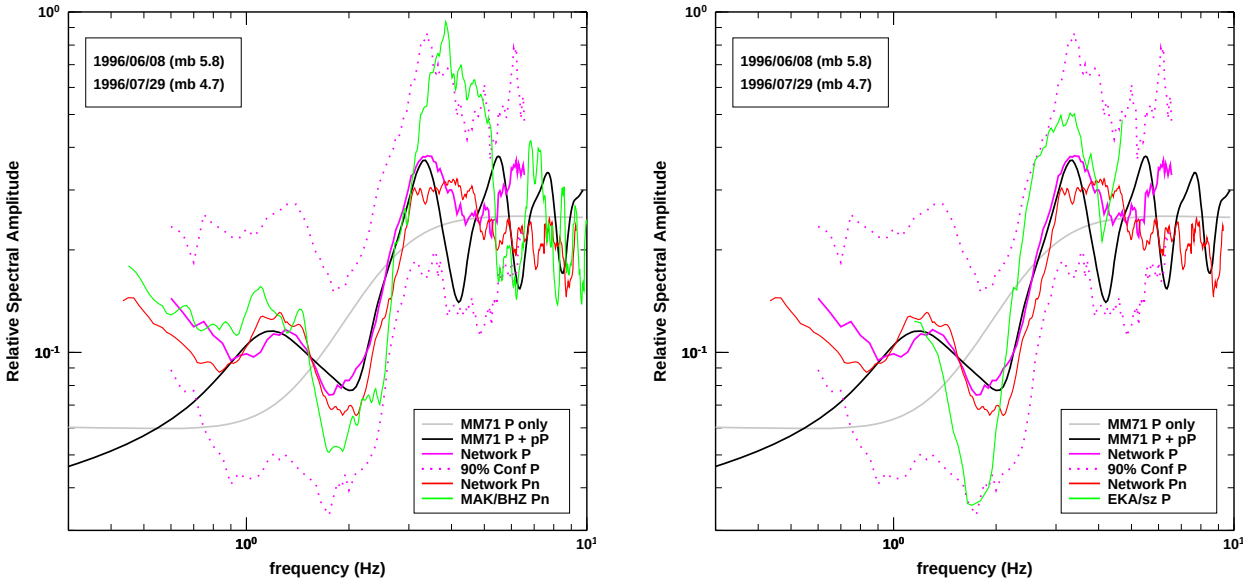

Figure 3. Empirical and model P and Pn relative spectra for the 1996/07/29 and 1996/06/08 LNTS explosions. The green curves represent the relative spectra of Pn at MAK (left) and P at EKA (right).

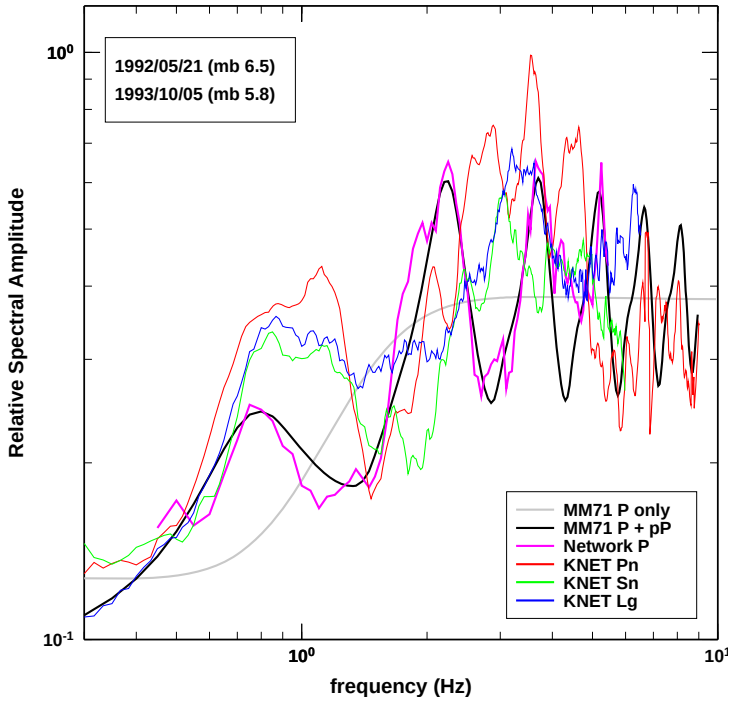

Figure 4. Model and empirical P, Pn, Sn, and Lg relative spectra for the 1993/10/05 to 1992/05/21 LNTS shots.

Figure 4 shows that the MM71 (P+pP) model fits the network-averaged P spectral ratio reasonably well from about 0.5 to 4.0 Hz. It also shows the Pn spectral ratio (red curve) averaged over 5 KNET stations with common recordings

of these two shots. Agreement between the Pn and P spectral ratios is not very good in this case, likely because only 5 stations with little azimuthal coverage are available. Nevertheless, some similar qualitative frequency dependence can be observed in both spectral ratios (e.g., common local maxima at about 0.7 Hz). Last, the Sn and Lg relative spectra in Figure 4 do not exhibit enhanced energy at lower frequencies compared to the Pn relative spectra (contrary to the effect observed in Figure 2 for the smaller/shallower 1996/07/29 tunnel shot).

Implications for Regional P/S Discriminants

To investigate regional P/S discrimination performance, we compare empirical spectral ratios of Pn/Sn and Pn/Lg to model predictions. In this case, differential attenuation of P and S waves must be treated. The attenuation coefficients estimated by Taylor et al. (2002) for station MAK are used here. Figure 5 shows Pn/Sn and Pn/Lg spectral ratios at MAK for the 1996 explosions and the 1999 earthquakes. The smaller events have less bandwidth because of the SNR threshold of 2.5. The solid and dashed gray curves show predictions of the modified Brune model for the 1999/01/30 and 1999/01/27 earthquakes. The shapes of these curves are due to differential attenuation of P and S phases and different P and S corner frequencies as functions of moment. Model spectral ratios for the earthquakes (gray curves) provide relatively good fits to the data, although there is no evidence in this case, nor some other studies (e.g., Walter and Taylor, 2002) that P/S is systematically lower for smaller earthquakes. The solid and dashed black curves show MM71 predictions for the explosions assuming the same source model for all phases, but with Sn and Lg corner frequency lower than for Pn by a factor of $v_s(S)/v_s(P)$. Differences in P/S spectral values between the two shots are due to differences in P and S corner frequencies (as suggested by Xie and Patton, 1999) as functions of yield and pP interference effects (cf. Figure 2). The offset between the gray and black curves is largely due to the ratio of P and S velocities in the Brune model. That is, the ratio of earthquake P/S spectral amplitudes at zero frequency is given by

$$\frac{S_P(0)}{S_S(0)} = \frac{R_{\theta\phi}^{(P)}}{R_{\theta\phi}^{(S)}}\left[\frac{v_s(S)^5 v_r(S)}{v_s(P)^5 v_r(P)}\right]^{1/2}. \qquad (6)$$

Using values from Taylor et al. (2002) of $R_{\theta\phi}^{(P)} = 0.44$ and $R_{\theta\phi}^{(S)} = 0.60$ for the average radiation pattern terms and $v_s(P) = 6100$, $v_r(P) = 5000$, $v_s(S) = 3526$, $v_r(S) = 2890$ (all in units of m/s) for the source and receiver P and S medium velocities, the expression in (6) equals 0.14. For comparison, the dotted black curves in each plot represent the P/S spectral ratios for explosions, assuming the same MM71 model (and corner frequencies) for P and S waves.

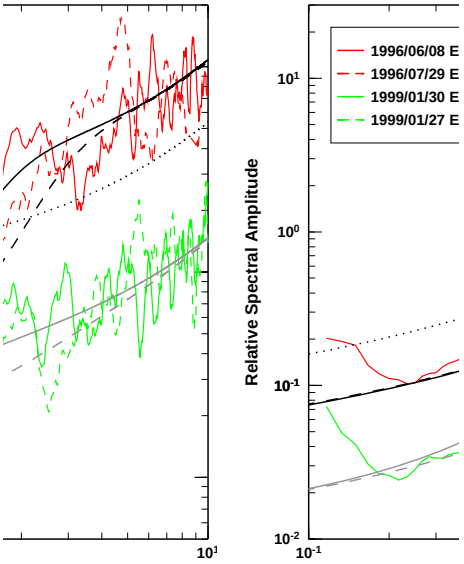

Figure 5. Empirical and model Pn/Sn (left frame) and Pn/Lg (right frame) spectral ratios for MAK BHZ recordings of the two 1996 explosions and two 1999 earthquakes at the LNTS.

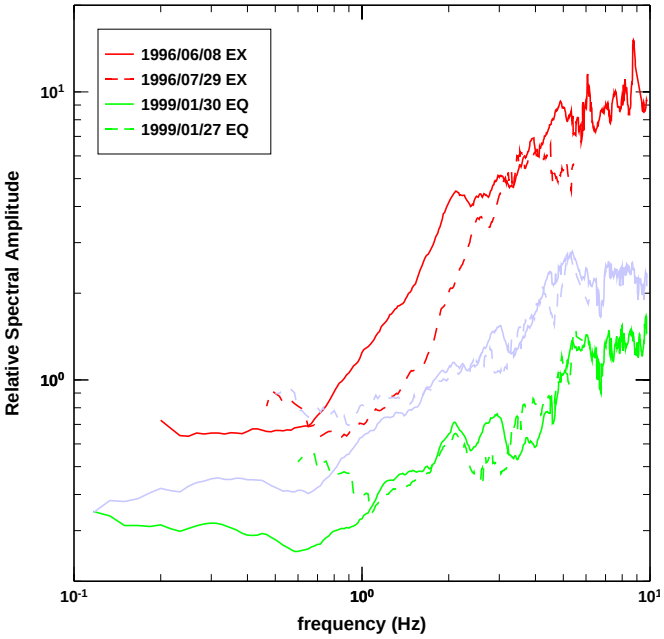

Figure 6. Network-averaged Pn/Sn spectral ratios for two 1996 LNTS explosions and two 1999 earthquakes with time windows that include (blue curves) or exclude (green curves) depth phases.

As an aside, Figure 6 shows that reflected phases can also affect P/S discriminants for earthquakes. Depicted are network-averaged Pn/Sn spectral ratios for the 1996 explosions and 1999 earthquakes at LNTS. The light blue curves represent the spectral ratios for earthquakes using a default velocity window for Pn (6.8 to 8.2 km/s), while the green curves are for a time window that excludes at least sPn at all stations. The results are yet to be corrected for station-dependent attenuation and site effects, but this does not affect the general conclusion regarding the potential impact of depth phases from earthquakes on Pn measurements, which can significantly affect P/S discrimination performance.

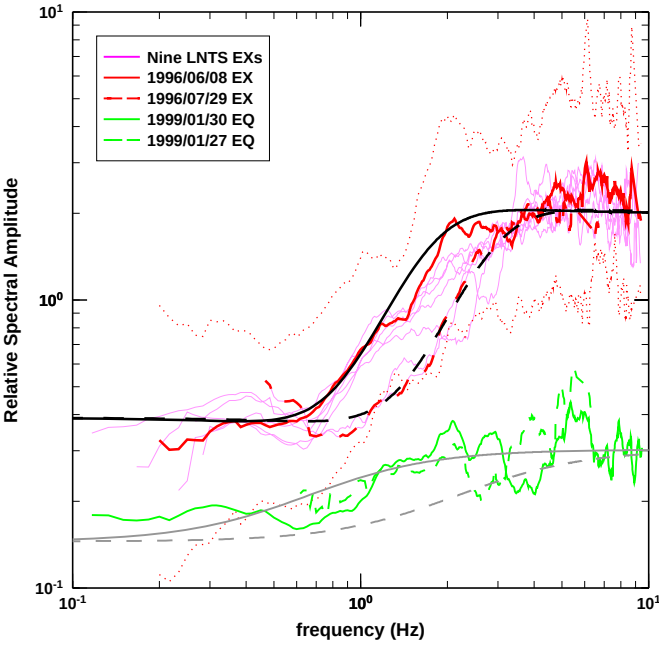

Figure 7. Network-averaged Pn/Sn spectral ratios, corrected for attenuation and station effects, for nine LNTS explosions and two 1999 earthquakes. Theoretical predictions of Pn/Sn ratios are shown for the 1996 shots and 1999 earthquakes (black and gray curves). The dotted red curves represent

As an example of recent results, Figure 7 shows Pn/Sn spectral ratios for nine LNTS explosions with regional data (magenta curves), the 1996 shots (red curves), and the 1999 earthquakes (green curves), using

preliminary attenuation and station corrections, and then network averaging. Model predictions are shown for the 1996 explosions and 1999 earthquakes (black and gray curves, respectively), which seem to adequately represent the data and indicate that the main effect of frequency-dependent P/S discrimination performance is due to different corner frequencies of P and S waves and stronger spectral shapes (including overshoot) for explosions than earthquake spectra. Note that we increased the explosion Pn corner frequencies by 30%, as was done by Murphy and Barker (2001), to obtain the model results. Also shown is the 90% confidence interval of Pn/Sn for the 1996/06/08 shot (dotted red curves), which illustrates the considerable variability of Pn/Sn spectral ratios at the various stations. We plan to investigate this variability using numerical simulations, and these source model parameterizations, during subsequent phases of this contract.

CONCLUSIONS AND RECOMMENDATIONS

Although these preliminary results are anecdotal at this point, and subject to revision after further investigations, there are some interesting observations. First, the modified Brune (1970) source model with corner frequency scaling as moment to -1/4 power seems to adequately predict spectral scaling for the earthquakes considered here and past observations in central Asia by several authors. Relative spectra of Pn, Sn, and Lg exhibit fairly minor differences over a frequency range of about 0.5 to 5.0 Hz, suggesting that the frequency dependence of P/S discrimination performance is not primarily due to earthquake source mechanisms, although the relative P and S wave velocities near the source are expected to affect P/S discrimination performance at all frequencies. As an ancillary comment, windows used to measure first P amplitudes for earthquakes should be designed to exclude depth phases, if possible.

Second, the modified MM71 P+pP model provides reasonably good fits up to about 3-4 Hz to empirical spectral ratios of P and Pn for LNTS explosions, if they are suitably averaged over stations and azimuths. Spectral effects of pP interference can be significant for teleseismic and regional phases. For LNTS explosions between mb 4.7 to 6.5, the main effect of destructive pP interference occurs between roughly 0.7 to 2.5 Hz. This cause of weak P amplitudes in this frequency range has been discussed at length by Lay (1991) and others, typically in the context of teleseismic P waves. Note that a relative pP amplitude of 0.5 produces a range of variations from the P-only MM71 model by a factor of three. It is interesting that the relative amplitudes of pP are the largest for the 1996/07/29 tunnel shot (A = 0.49) and the 1993/10/05 shaft shot (A = 0.48), which seems to have been somewhat overburied. Note that the average pP relative amplitudes estimated by Murphy and Barker (2001) and Murphy (2005) for LNTS explosions between 1976 and 1992 are 0.50 for the tunnel shots and 0.18 for the shaft shots. It is tempting to speculate that the tunnel and overburied shots may have produced much weaker spallation, leading to stronger (more linear) reflections of pP. This effect, along with strong enhancement of regional S waves in this frequency range for smaller/shallower shots may contribute to poorer regional P/S discrimination at frequencies below about 3 Hz. However, as noted by Xie and Patton (1999), frequency-dependent performance of regional P/S discriminants appears to be primarily due to differences in corner frequencies of P and S waves and spectral shape (including overshoot) for explosions.

As shown in the Lop Nor Advanced Concept Demonstration (e.g., Bahavar et al., 2004), Pn/Sn discrimination results using 3-component records in the 4-6 Hz band are all very comparable for nine actual nuclear explosions (mb 4.7 to 6.5) and simulated explosions scaled down to mb 3.0. There is no evidence, empirically or theoretically, that this should not be true for P/S measurements above the Pn corner frequency for explosions, where discrimination performance seems to saturate. However, at lower frequencies there is evidence that explosions can have enhanced S wave energy relative Pn, leading to poorer discrimination. Note that the Brune and MM71 models we used here both predict that the ratio of asymptotic high-frequency to low-frequency limits of P/S behave according to the ratio of the P to S corner frequencies squared. Using the geologic parameters considered here for LNTS, the ratio of asymptotic limits of high-frequency to low-frequency P/S is about 2 for earthquakes and about 5 for explosions (cf. Figure 7). Much more work is needed to examine this behavior for other regions and many more events, but a geophysical

understanding of frequency-dependent P/S discrimination performance seems attainable, which could be utilized to predict performance, on average, for regions with sufficient geologic information. Encouraging results thus far are (1) a better understanding of why P/S discriminants do not perform as well at lower frequencies and (2) that application of regional P/S discriminants should be limited to frequencies above the Pn corner frequency for explosions, which can be computed, at least in principle, if adequate information is available regarding the explosion yield, depth, and near-source geology. Considerably more work is required to understand regional phase variability due to path (scattering) and station effects.

Future plans include (1) analysis of more earthquakes near Lop Nor; (2) application of numerical simulations to explore geophysical path and station effects on the variability of individual phases for LNTS events, using the source model parameterizations developed thus far; and (3) similar investigations at other nuclear test sites. More work is certainly needed to better understand source excitation and scattering effects for regional S waves from explosions.

ACKNOWLEDGMENTS

We are grateful to Howard Patton, Jiakang Xie, and Gary McCartor for many useful discussions.

REFERENCES

Bahavar, B., B. Barker, G. Beall, I. Bondar, D. Brumbaugh, M. Fisk, J. Hanson, H. Israelsson, B. Kohl, Y.-L. Kung, J. Murphy, R. North, V. Oancea and J. Stevens (2004). Seismic calibration of Lop Nor, China test site region for improved regional monitoring, Editor J. Bennett, Science Applications International Technical Report, SAIC-04/2208.

Brune, J. N. (1970). Tectonic stress and the spectra of seismic shear waves from earthquakes, *J. Geophys. Res.*, **75**, 4997-5009.

Cong, L., J. Xie and B. J. Mitchell (1996). Excitation and propagation of Lg from earthquakes in central Asia with implications for explosion/earthquake discrimination, *J. Geophys. Res.*, 101, 27,779-27,789.

Denny, M. D. and L. R. Johnson (1991). The explosion seismic source function: models and scaling laws reviewed, *Explosion Source Phenomenology, Geophysical Monograph*, 65, 1-24.

Hanks, T. and H. Kanamori (1979). A moment-magnitude scale, *J. Geophys. Res.*, 84, 2348-2350.

Lay, T. (1991). The teleseismic manifestation of pP: problems and paradoxes, *Explosion Source Phenomenology, Geophysical Monograph*, 65, 109-125.

Matzko, J. R. (1994). Geology of the Chinese nuclear test site near Lop Nor, Xinjiang Uygur Autonomous Region, China, *Engineering Geology*, 36, 173-181.

Mayeda, K. and W. R. Walter (1996). Moment, energy, stress drop, and source spectra of Western United States earthquakes from regional coda envelopes, *J. Geophys. Res.*, 101, 11,195-11,208.

Mueller, C. S. and J. R. Murphy (1971). Seismic characteristics of underground nuclear detonations Part I: seismic spectrum scaling, *Bull. Seism. Soc. Am.*, 61, 1675-1692.

Murphy, J. R. and B. W. Barker (2001). Application of network-averaged teleseismic P-wave spectra to seismic yield estimation of underground nuclear explosions, *Pure and Appl. Geophys., Special Edition on Monitoring the Comprehensive Nuclear-Test-Ban Treaty: Source Processes and Explosion Yield Estimation*, 158, 2123-2171.

Nuttli, O. W. (1983). Average seismic source-parameter relations for mid-plate earthquakes, *Bull. Seism. Soc. Am.*, 73, 519-535.

Taylor, S. R., A. A. Velasco, H. E. Hartse, W. S. Phillips, W. R. Walter, and A. J. Rodgers (2002). Amplitude corrections for regional seismic discriminants, *Pure and Appl. Geophys., Special Edition on Monitoring the Comprehensive Nuclear-Test-Ban Treaty: Seismic Event Discrimination and Identification*, 159, 623-650.

Walter, W. R. and S. R. Taylor (2002). A Revised Magnitude and Distance Amplitude Correction (MDAC2) Procedure for Regional Seismic Discriminants: Theory and Testing at NTS, *UCRL-ID-146882, LA-UR-02-1008*.

Xie, J. and H. J. Patton (1999). Regional phase excitation and propagation in the Lop Nor region of central Asia and implications for P/Lg discriminants, *J. Geophys. Res.*, 104, 941-954.